JOURNAL OF SOLID STATE CHEMISTRY 112, 15–21 (1994)

Mixed Valent Molybdenum Monophosphates with an Intersecting Tunnel Structure: $A_3O_2(MoO)_4(PO_4)_4$ (A = Rb, Tl)

M. M. Borel, A. Leclaire, A. Guesdon, A. Grandin, and B. Raveau

Laboratoire CRISMAT URA 1318 associé au CNRS, ISMRA/Université de Caen, Boulevard du Maréchal Juin, 14050 Caen Cedex, France

Received July 1, 1993; in revised form October 18, 1993; accepted October 22, 1993

New mixed valent monophosphates $A_3O_2(MoO)_4(PO_4)_4$ with an intersecting tunnel structure have been isolated for A = Rb, Tl. The structure of the Rb-phase has been solved from a single crystal X-ray diffraction study. It crystallizes in the space group $C222_1$ with $a = 14.222(1)$ Å, $b = 14.223(1)$ Å, and $c = 19.227(4)$ Å. The structure is in fact closely related to that of the Mo(V) monophosphate $K_2O(MoO)_2(PO_4)_2$. It consists of similar double layers $[Mo_2P_2O_{11}]_\infty$ parallel to (001) and it is deduced from this Mo(V) monophosphate by a rotation of one double layer out of two of 180°, so that it can be described as a chemical twin of the phosphate $K_2O(MoO)_2(PO_4)_2$. The geometry of the MoO_6 octahedra is characteristic of Mo(V) in spite of the mixed valent Mo(V)–Mo(VI). The bond valence calculations suggest a delocalization of the electron between the two octahedra of the bioctahedral units Mo_2O_{11}. © 1994 Academic Press, Inc.

INTRODUCTION

Recently a new series of Mo(V) monophosphates with the generic formula $A_2O(MoO)_2(PO_4)_2$ was synthesized for A = K, Rb and Tl (1). These compounds, which are isotypic with the niobium arseniates $A_2O(NbO)_2(AsO_4)_2$ with A = K, Rb, Tl, Cs (2, 3), exhibit an intersecting tunnel structure. The dimensions of some of the cavities seem to be significantly larger in the arseniates than in the phosphates. Consequently, the isotypic cesium molybdenophosphate could only be synthesized for a cationic deficiency, according to the formula $Cs_3O_2(MoO)_4(PO_4)_4$ (4). A first interesting characteristic of the latter phase is the ordered occupancy of the tunnels, two sites being fully occupied by Cs^+, the third one being empty owing to the too large size of Cs^+. A second remarkable feature of this phase is the mixed valency of molybdenum Mo(V)–Mo(VI), which shows for the first time the possibility of Mo(VI) to exhibit the same geometry as Mo(V), i.e., to be off-centered in the same way in an almost regular O_6 octahedron forming short molybdenyl Mo–O bonds. In order to understand this peculiar behavior, attempts were made to synthesize Mo(V)–Mo(VI) phosphates with a similar formulation, but replacing cesium by smaller cations like rubidium or thallium. We report here on new mixed valent molybdenum monophosphates $A_3O_2(MoO)_4(PO_4)_4$ with A = Rb, Tl with an original intersecting tunnel structure that can be described as a chemical twin of the monophosphate $A_2O(MoO)_2(PO_4)_2$ and $Cs_3O_2(MoO)_4(PO_4)_4$.

SYNTHESIS

The growth of single crystals of the phosphates $A_3O_2(MoO)_4(PO_4)_4$ (A = Rb and Tl) was performed in two steps from a mixture of nominal composition $AMo_2P_2O_{11}$ (A = Rb and Tl). First an adequate mixture of A_2CO_3, $H(NH_4)_2PO_4$, and MoO_3 was heated in air to 673 K to eliminate CO_2, H_2O, and NH_3. In a second step 0.17 mole of molybdenum was added to the intermediate composition $AMo_{1.833}P_2O_{11}$; the finely ground product placed in an alumina crucible was heated in an air evacuated silica ampoule at 1000 K for 12 hr. The sample was then cooled slowly ($3°hr^{-1}$) to 800 K.

From the resulting mixture we have extracted some black crystals whose composition $A_3O_2(MoO)_4(PO_4)_4$ was confirmed by microprobe analysis in agreement with the structure determination.

The synthesis of pure powder samples of these phosphates $A_3O_2(MoO)_4(PO_4)_4$ was performed in a similar way in two steps but starting from the exact stoichiometric composition. The second step was carried out at 950 K for 1 day and the compounds were finally quenched at room temperature. The results were a dark green powder.

The powder X-ray diffractograms registered with a PW3710 Philips diffractometer were indexed in an orthorhombic cell (Table I) in agreement with the parameters obtained from the single crystal study (Table 2).

STRUCTURE DETERMINATION

Two black crystals were selected for the structure determination with dimensions 0.115 × 0.103 ×0.040 mm and 0.026 × 0.026 × 0.045 mm for rubidium and thallium

0022-4596/94 $6.00

phases, respectively. The cell parameters were determined and refined by diffractometric techniques at 294 K with a least-squares refinement based upon 25 reflections with $18° < \theta < 22°$ (Table 2). The almost equal a and b parameters led us to believe that the cell was tetragonal. The study of the $\pm h \pm k$ 2 reflections shows first that the variation of the intensity of the *hkl*, *-hkl*, *h-kl* and *-h-kl* reflections is less than 8%, and second that the variation of the intensities between the *hkl* set and the corresponding *khl* set rises to 30%. So there are only two mirrors running respectively along **a** and **b**, and no A_4 axis and no mirrors along ⟨110⟩ were found. One can admit then that the Laue symmetry class is *mmm* instead of $4/m$ or $4/mmm$, but the structure should be pseudotetragonal.

The cell parameters (a_o, b_o, c_o) of these two orthorhombic phosphates can be related to those of the monoclinic cell $a_m b_m c_m$ that characterizes the monophosphate $A_2O(MoO)_2(PO_4)_2$ or $Cs_3O_2(MoO)_4(PO_4)_4$ (Table 2). One indeed observes the following relations: $\mathbf{c}_o \approx \mathbf{c}_m$ and $\mathbf{a}_o \approx \mathbf{a}_m + \mathbf{b}_m$.

The data were collected on an Enraf–Nonius CAD4 diffractometer with the data collection parameters reported in Table 3. Unfortunately for $Tl_3O_2(MoO)_4(PO_4)_4$ the small number of reflections (350) that could be collected did not allow the structure to be solved. The reflections were collected for Lorentz, polarization, absorption, and secondary extinction effects.

The structure was solved by the heavy atom method with the space group $C222_1$ in agreement with the observed extinctions: $h + k = 2n + 1$ for all the *hkl* and $l = 2n + 1$ for 00*l*. The refinement of the atomic coordinates and their thermal anisotropic factors led to $R = 0.029$ and $R_w = 0.031$ and to the atomic parameters shown in Table 4.

The refinement of the enantiomorphic structure led to larger values of the R and R_w factors.

DESCRIPTION OF THE STRUCTURE AND DISCUSSION

The structure of this new mixed valent molybdenum phosphate is characterized by $[Mo_2P_2O_{11}]_\infty$ single layers of polyhedra parallel to (001) practically identical (Fig. 1) to those observed in the monophosphates $A_2O(MoO)_2(PO_4)_2$ or $Cs_3O_2(MoO)_4(PO_4)_4$ (1–4). As in the latter

TABLE 1
Interreticular Distances for $Rb_3O_2(MoO)_4(PO_4)_4$

h k l	d_{cal}(Å)	d_{obs}(Å)	I/I_0	*h k l*	d_{cal}(Å)	d_{obs}(Å)	I/I_0
0 2 0	7.111	7.110	25.9	1 3 7	2.344	2.346	8.3
2 0 0	7.111			3 1 7	2.344		
0 2 1	6.670	6.657	1.6	1 1 8	2.338	2.339	8.1
2 0 1	6.670			3 3 6	2.316	2.317	2.9
0 2 2	5.717	5.712	15.8	0 6 2	2.302	2.303	2.7
2 0 2	5.717			6 0 2	2.302		
1 1 3	5.405	5.406	0.7	3 5 3	2.280	2.278	10.9
0 0 4	4.807	4.806	18.6	5 3 3	2.280		
0 2 3	4.761	4.762	14.0	0 2 8	2.277		
2 0 3	4.761			2 0 8	2.277		
1 3 0	4.498	4.499	18.0	2 6 0	2.249	2.247	4.9
3 1 0	4.498			6 2 0	2.249		
1 3 1	4.379	4.379	56.4	2 6 1	2.234	2.233	3.4
3 1 1	4.379			6 2 1	2.234		
1 1 4	4.337	4.339	33.5	0 6 3	2.223	2.223	2.0
1 3 2	4.074	4.075	2.6	6 0 3	2.223		
3 1 2	4.074			3 5 4	2.175	2.175	11.5
0 2 4	3.982	3.980	3.5	5 3 4	2.175		
2 0 4	3.982			0 4 7	2.174		
2 2 3	3.956	3.958	3.3	4 0 7	2.174		
1 3 3	3.682	3.684	10.9	2 2 8	2.168	2.168	5.5
3 1 3	3.682			0 6 4	2.168	2.126	4.2
1 1 5	3.592	3.597	3.4	6 0 4	2.126		
2 2 4	3.475	3.476	6.1	3 3 7	2.125		
0 2 5	3.383	3.385	32.7	4 4 5	2.104	2.104	2.4
2 0 5	3.383			1 5 6	2.104		
0 4 2	3.335	3.335	4.8	5 1 6	2.104		
4 0 2	3.335			1 1 9	2.090	2.090	2.6
2 4 1	3.138	3.137	100.0	3 5 5	2.060	2.060	1.9
4 2 1	3.138			5 3 5	2.060		

TABLE 1—*Continued*

h k l	d_{cal}(Å)	d_{obs}(Å)	I/I_0	*h k l*	d_{cal}(Å)	d_{obs}(Å)	I/I_0
0 4 3	3.109	3.110	78.7	0 2 9	2.046	2.047	3.5
4 0 3	3.109			2 0 9	2.046		
1 1 6	3.053	3.054	4.3	0 6 5	2.018	2.019	14.9
2 4 2	3.019	3.021	43.8	6 0 5	2.018		
4 2 2	3.019			1 7 0	2.011	2.013	6.6
1 3 5	2.923	2.925	20.3	5 5 0	2.011		
3 1 5	2.923			7 1 0	2.011		
0 2 6	2.922			0 4 8	1.991	1.992	2.8
2 0 6	2.922			4 0 8	1.991		
2 4 3	2.849	2.850	5.1	4 4 6	1.978	1.978	38.1
4 2 3	2.849			4 6 0	1.972	1.973	19.4
1 5 0	2.789	2.790	1.7	6 4 0	1.972		
5 1 0	2.789			1 5 7	1.957	1.958	14.5
1 5 1	2.760	2.760	3.9	5 1 7	1.957		
5 1 1	2.760			3 3 8	1.953	1.952	5.9
1 5 2	2.679	2.679	4.1	2 6 5	1.941	1.942	5.9
5 1 2	2.679			6 2 5	1.941		
2 4 4	2.652	2.654	12.7	3 5 6	1.941		
4 2 4	2.652			5 3 6	1.941		
0 4 5	2.611	2.611	15.6	1 3 9	1.930	1.931	6.8
4 0 5	2.611			3 1 9	1.930		
1 3 6	2.610			1 7 3	1.919	1.919	5.2
3 1 6	2.610			5 5 3	1.919		
1 5 3	2.558	2.557	6.7	7 1 3	1.919		
5 1 3	2.558			2 4 8	1.917		
3 3 5	2.527	2.526	1.3	4 2 8	1.917		
2 4 5	2.451	2.452	5.9	4 6 3	1.885	1.885	0.4
4 2 5	2.451			6 4 3	1.885		
2 2 7	2.411	2.410	1.3	3 7 1	1.859	1.856	6.9
3 5 2	2.364	2.366	1.3	7 3 1	1.859		
5 3 2	2.364						

monophosphates, each monophosphate group shares its four apices with MoO_6 octahedra, whereas each MoO_6 shares four of its apices with PO_4 tetrahedra, and one with another MoO_6 octahedron, the sixth one being free. One also recognizes from the projection of the $[Mo_2P_2O_{11}]_\infty$ monolayer along **c** (Fig. 1) the bioctahedral units Mo_2O_{11} that form the $Mo_2P_2O_{15}$ units with the PO_4 tetrahedra (Fig. 2), as previously described for the two other series of monophosphates (1–4).

In fact the structure of the monophosphate $Rb_3O_2(MoO)_4(PO_4)_4$ differs from that of the $K_2O(MoO_4)_2(PO_4)_2$-type series by the stacking of the $[Mo_2P_2O_{11}]_\infty$ layers along **c**. The relationships between the two host lattices are easily understood from their projections along **a** (Fig. 3a) and along ⟨110⟩ (Fig. 3b), respectively. Both frameworks consist of similar slabs labelled A built up from the stacking of two single $[Mo_2P_2O_{11}]_\infty$ layers along **c** forming S-shaped tunnels. The thickness of these slabs determines the periodicity c in the $K_2O(MoO)_2(PO_4)_2$-type structure (Fig. 3b), whereas one slab out of two is rotated 180° around **a** in the $Rb_3O_2(MoO)_4(PO_4)_4$ structure (Fig. 3a), leading to the sequence A–A′–A–A′. Thus two succes-

TABLE 2
Crystallographic Parameters

Compounds	a(Å)	b(Å)	c(Å)	β(°)	V(Å^3)
$Rb_3O_2(MoO)_4(PO_4)_4$	14.222(1)	14.223(1)	19.227(4)		3889
$Tl_3O_2(MoO)_4(PO_4)_4$	14.217(2)	14.218(8)	19.241(3)		3889
$Cs_3O_2(MoO)_4(PO_4)_4$	10.134(1)	10.104(1)	9.952(1)	100.44(1)	1002
$K_2O(MoO)_2(PO_4)_2$	9.867(2)	10.122(1)	9.903(2)	97.95(2)	979
$Rb_2O(MoO)_2(PO_4)_2$	9.88(3)	10.16(3)	9.93(2)	97.6(2)	988
$Tl_2O(MoO)_2(PO_4)_2$	9.945(1)	10.156(1)	9.974(2)	97.64(1)	998

TABLE 3
Summary of Crystal Data, Intensity Measurements, and Structure Refinement Parameters

$Rb_3O_2(MoO)_4(PO_4)_4$	
Crystal data	
Space group	$C222_1$
Cell dimensions (Å)	a = 14.222(1)
	b = 14.223(1)
	c = 19.227(4)
Volume (Å)^3	3889(1)
Z	8
d_{calc}	3.81
d_{mes}	3.70
Intensity measurements	
$\lambda(MoK\alpha)$	0.71073
Scan mode	$\omega - 5/3\ \theta$
Scan width (°)	1. + 0.35 tan θ
Slit aperture (mm)	1.1 + tan θ
max θ (°)	45
Standard reflections	3 (every 3000 sec)
Reflections with $I > 3\sigma$	2523
Measured reflections	8581
Range h	0 → 27
k	0 → 27
l	0 → 36
μ (mm^{-1})	10.1
Structure solution and refinement	
Parameters refined	300
Agreement factors	R = 0.029 R_2 = 0.031
Weighting scheme	$w = f(\sin\theta/\lambda)$
Δ/σ max	<0.03
$\Delta\rho$ (e Å^{-3})	0.4

sive slabs A and A′ can be described as being deduced from each other by a chemical twinning. As a consequence, the projections of the two structures along **c** (Fig. 4) are different in spite of their great similarity. One ob-

TABLE 4
Positional Parameters and Their Estimated Standard Deviations

Atom	x	y	z	B(A^2)
Rb(1)	0.05358(9)	0.44118(9)	0.12649(7)	2.04(2)
Rb(2)	0.2081(2)	0	0.5	3.10(4)
Rb(3)	0.44128(9)	0.44653(9)	0.37644(7)	2.05(2)
Rb(4)	0.5	0.2084(2)	0.25	3.03(4)
Mo(1)	0.19029(5)	0.32595(5)	0.31033(4)	0.474(9)
Mo(2)	0.17406(5)	0.19026(5)	0.06031(4)	0.493(9)
Mo(3)	0.42511(5)	0.18052(5)	0.06374(4)	0.500(9)
Mo(4)	0.18057(5)	0.07492(5)	0.31366(4)	0.494(9)
P(1)	0.0526(2)	0.2087(2)	0.4196(1)	0.51(3)
P(2)	0.3451(1)	0.1996(2)	0.4100(1)	0.47(3)
P(3)	0.3005(2)	0.3450(2)	0.1601(1)	0.56(3)
P(4)	0.2917(2)	0.0530(2)	0.1696(1)	0.47(3)
O(1)	0.1026(5)	0.3734(5)	0.2637(4)	1.3(1)
O(2)	0.1783(4)	0.2008(5)	0.2870(3)	0.70(9)
O(3)	0.1098(5)	0.2929(5)	0.3950(4)	1.0(1)
O(4)	0.2959(5)	0.3436(4)	0.2403(3)	0.8(1)
O(5)	0.2192(5)	0.4535(5)	0.3576(4)	1.1(1)
O(6)	0.3027(5)	0.2869(4)	0.3773(4)	1.1(1)
O(7)	0.1262(5)	0.1034(5)	0.0135(4)	1.1(1)
O(8)	0.0479(5)	0.2190(5)	0.1073(3)	0.9(1)
O(9)	0.2065(5)	0.1099(5)	0.1445(4)	1.0(1)
O(10)	0.1558(4)	0.2954(5)	−0.0094(3)	1.0(1)
O(11)	0.2990(5)	0.1780(5)	0.0366(3)	0.8(1)
O(12)	0.2117(4)	0.3032(5)	0.1276(4)	1.1(1)
O(13)	0.4685(5)	0.0966(5)	0.0127(4)	1.2(1)
O(14)	0.4484(4)	0.2910(5)	0.0004(3)	0.8(1)
O(15)	0.5509(4)	0.1967(6)	0.1142(3)	1.1(1)
O(16)	0.3869(5)	0.0956(5)	0.1465(4)	0.9(1)
O(17)	0.3896(4)	0.2944(5)	0.1376(3)	0.8(1)
O(18)	0.0959(5)	0.0307(5)	0.2628(4)	1.4(1)
O(19)	0.0935(5)	0.1133(5)	0.3967(4)	0.8(1)
O(20)	0.1954(6)	−0.0499(5)	0.3632(3)	1.1(1)
O(21)	0.2919(4)	0.0507(4)	0.2502(4)	0.7(1)
O(22)	0.2945(5)	0.1105(4)	0.3876(3)	0.9(1)

Note. Anisotropically refined atoms are given in the form of the isotropic equivalent displacement parameter defined as $B = \frac{4}{3} \Sigma_i \Sigma_j \mathbf{a}_i \cdot \mathbf{a}_j \cdot \beta_{ij}$.

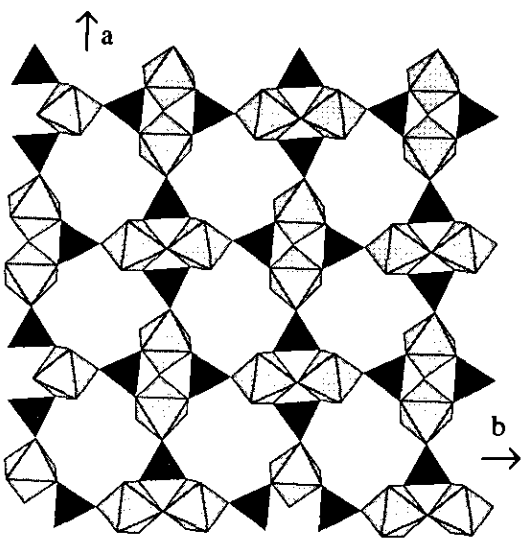

FIG. 1. $[Mo_2P_2O_{11}]_\infty$ layer parallel to the (001) plane.

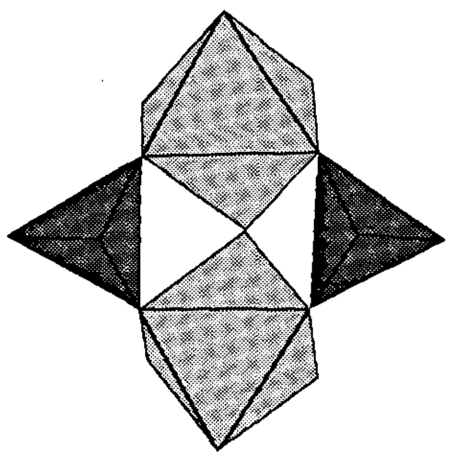

FIG. 2. $[Mo_2P_2O_{15}]$ unit.

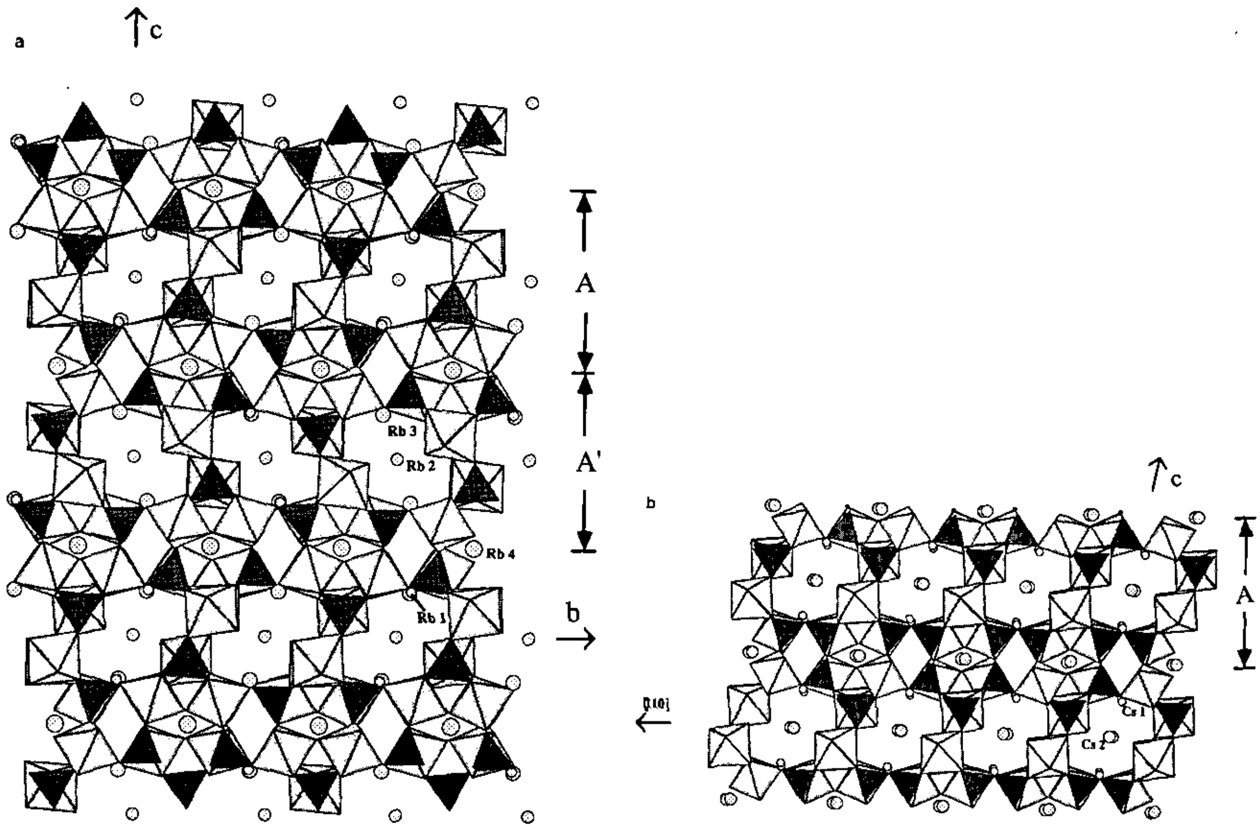

FIG. 3. Projection of host lattices (a) for $Rb_3O_2(MoO)_4(PO_4)_4$ along **a** and (b) for $Cs_3O_2(MoO)_4(PO_4)_4$ along ⟨110⟩.

tains zigzag tunnels along **c** in the Rb-monophosphate $Rb_3O_2(MoO)_4(PO_4)_4$ (Fig. 4a), whereas straight tunnels are observed in the monophosphate $K_2O(MoO)_2$ $(PO_4)_2$ (Fig. 4b).

The geometry of the PO_4 tetrahedra and of the MoO_6 octahedra is very similar to that observed for K_2O $(MoO_4)_2(PO)_2$ and $Cs_3O_2(MoO)_4(PO_4)_4$. The PO_4 tetrahedra have the classical geometry of monophosphate groups. The O_6 octahedra are almost regular, but the molybdenum atom is off-centered inside its octahedron toward the free oxygen atom (Table 5). As a result one observes one abnormally short Mo–O distance ranging

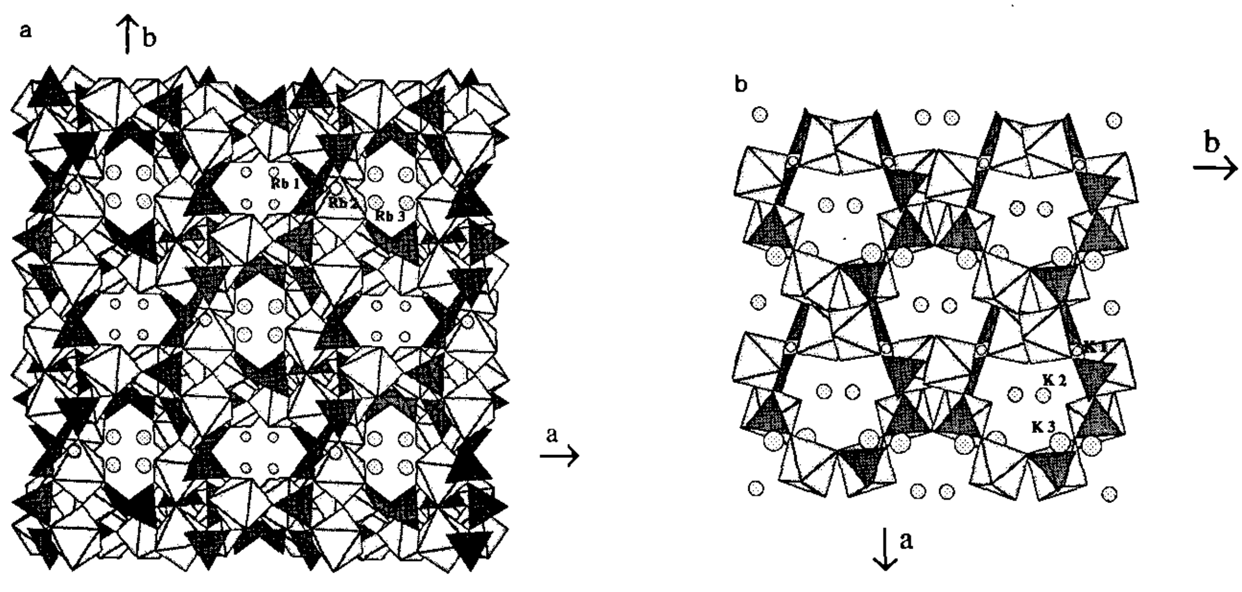

FIG. 4. (a) $Rb_3O_2(MoO)_4(PO_4)_4$ zigzag tunnels along **c**; (b) $K_2O(MoO)_2(PO_4)_2$ straight tunnels along **c**.

from 1.663 to 1.677 Å, corresponding to the free oxygen atom, as in the Mo(V) phosphate, whereas the opposite Mo–O distance is much longer (2.127 to 2.214 Å). The equatorial Mo–O distances are intermediate: three of them exhibit a mean value of 2.04 Å, characteristic of the Mo–O–P bond in Mo(V) phosphates, whereas the fourth one that corresponds to a Mo–O–Mo bond is significantly shorter, ranging from 1.843 to 1.868 Å. Bond valence calculations using the Zachariasen curve [5] suggest that no ordering of the Mo(V) and Mo(VI) species appears, i.e., that one electron is delocalized between the two corner-sharing octahedra of the Mo_2O_{11} units exactly as in $Cs_3O_2(MoO)_4(PO_4)_4$. One indeed obtains mean valences of 5.41 for Mo(1), 5.5 for Mo(2), and 5.3 for Mo(3) and Mo(4).

An interesting feature deals with the positions of the interpolated cations Rb^+ in tunnels that can be compared to those of potassium in the $K_2O(MoO)_2(PO_4)_2$ structure. In both structures the interpolated cations do not sit at the intersection of the tunnels. Among the four independent rubidium sites, two sites Rb(1) and Rb(3) correspond to the K(2) sites, whereas the two other sites Rb(2) and Rb(4) correspond to the K(1) sites. The Rb(1) and Rb(3) ions are located in the tunnels waving along **c**. The nine oxygen

TABLE 5
Distances (Å) and Angles (°) in the Polyhedra in $Rb_3O_2(MoO)_4(PO_4)_4$

Mo(1)	O(1)	O(2)	O(3)	O(4)	O(5)	O(6)
O(1)	1.677(8)	2.72(1)	2.77(1)	2.82(1)	2.70(1)	3.79(1)
O(2)	101.0(3)	1.843(7)	2.64(1)	2.78(1)	3.89(1)	2.77(1)
O(3)	95.8(4)	85.4(3)	2.044(7)	4.05(1)	2.86(1)	2.77(1)
O(4)	98.4(4)	91.5(3)	165.8(3)	2.033(7)	2.95(1)	2.76(1)
O(5)	91.7(3)	166.2(3)	87.9(3)	92.1(3)	2.070(8)	2.68(1)
O(6)	170.9(3)	88.0(3)	83.0(3)	83.0(3)	79.2(3)	2.127(8)
Mo(2)	O(7)	O(8)	O(9)	O(10)	O(11)	O(12)
O(7)	1.673(8)	2.68(1)	2.77(1)	2.80(1)	2.71(1)	3.79(1)
O(8)	91.6(3)	2.050(8)	2.83(1)	2.93(1)	3.87(1)	2.65(1)
O(9)	96.1(4)	87.7(3)	2.035(8)	4.03(1)	2.64(1)	2.77(1)
O(10)	97.9(4)	91.9(3)	166.1(3)	2.024(8)	2.78(1)	2.75(1)
O(11)	100.9(3)	166.4(3)	85.7(3)	91.7(3)	1.843(7)	2.79(1)
O(12)	170.2(3)	78.6(3)	83.3(3)	82.9(3)	88.8(3)	2.131(8)
Mo(3)	O(11)	O(13)	O(14)	O(15)	O(16)	O(17)
O(11)	1.868(7)	2.71(1)	2.75(1)	3.89(1)	2.72(1)	2.86(1)
O(13)	100.2(4)	1.663(8)	2.79(1)	2.69(1)	2.83(1)	3.87(1)
O(14)	90.2(3)	98.1(4)	2.016(8)	2.95(1)	4.05(1)	2.77(1)
O(15)	166.7(3)	92.1(4)	93.2(3)	2.049(7)	2.81(1)	2.72(1)
O(16)	87.2(3)	97.6(4)	164.3(3)	86.0(3)	2.070(7)	2.83(1)
O(17)	88.5(3)	171.2(3)	81.6(3)	79.2(3)	82.8(3)	2.213(7)
Mo(4)	O(2)	O(18)	O(19)	O(20)	O(21)	O(22)
O(2)	1.863(7)	2.73(1)	2.73(1)	3.86(1)	2.77(1)	2.85(1)
O(18)	100.8(4)	1.674(8)	2.83(1)	2.65(1)	2.81(1)	3.80(1)
O(19)	87.1(3)	96.8(4)	2.093(7)	2.81(1)	4.09(1)	2.87(1)
O(20)	166.8(3)	91.2(4)	86.1(3)	2.026(8)	2.94(1)	2.72(1)
O(21)	90.6(3)	98.4(4)	164.8(3)	93.1(3)	2.028(8)	2.78(1)
O(22)	88.3(3)	170.9(4)	83.3(3)	79.8(3)	81.6(3)	2.214(7)

P(1)	O(3)	O(8[i])	O(14[ii])	O(19)
O(3)	1.523(8)	2.48(1)	2.49(1)	2.57(1)
O(8[i])	108.7(5)	1.527(7)	2.51(1)	2.51(1)
O(14[ii])	108.3(4)	109.2(4)	1.553(8)	2.49(1)
O(19)	113.8(4)	109.9(5)	107.0(4)	1.540(8)
P(2)	O(6)	O(10[ii])	O(15[iii])	O(22)
O(6)	1.517(8)	2.54(1)	2.45(1)	2.52(1)
O(10[ii])	111.9(5)	1.553(8)	2.51(1)	2.49(1)
O(15[iii])	106.1(5)	108.0(4)	1.550(8)	2.52(1)
O(22)	112.2(4)	108.5(5)	110.2(5)	1.520(7)

TABLE 5—*Continued*

P(3)	O(4)	O(12)	P(17)	O(20^{iv})
O(4)	1.542(8)	2.54(1)	2.48(1)	2.51(1)
O(12)	111.6(5)	1.531(8)	2.54(1)	2.48(1)
O(17)	108.3(4)	112.8(4)	1.520(7)	2.52(1)
O(20^{iv})	107.6(4)	106.6(5)	109.9(5)	1.562(8)

P(4)	O(5^{v})	O(9)	O(16)	O(21)
O(5^{v})	1.516(8)	2.46(1)	2.53(1)	2.50(1)
O(9)	107.7(5)	1.535(8)	2.58(1)	2.51(1)
O(16)	110.9(5)	113.2(4)	1.549(8)	2.49(1)

Rb(1)–O(1)	= 2.895(8)	Rb(3)–O(5)	= 3.180(8)
–O(1^{i})	= 3.212(9)	–O(6)	= 3.006(8)
–O(3^{i})	= 3.165(8)	–O(7^{ii})	= 2.893(9)
–O(8)	= 3.183(8)	–O(7^{iv})	= 3.221(8)
–O(12)	= 2.984(8)	–O(9^{iv})	= 3.159(8)
–O(13^{vi})	= 3.338(8)	–O(17^{iii})	= 3.246(8)
–O(13^{vii})	= 2.986(8)	–O(18^{ix})	= 3.324(9)
–O(16^{vi})	= 3.254(7)	–O(18^{iv})	= 2.979(9)
–O(22^{iv})	= 3.247(8)	–O(19^{ix})	= 3.235(8)
Rb(2)–O(19)	= 3.033(8)	Rb(4)–O(4)	= 3.487(8)
–O(19^{viii})	= 3.033(8)	–O(4^{iii})	= 3.487(8)
–O(20)	= 2.729(8)	–O(15)	= 2.715(8)
–O(20^{viii})	= 2.729(8)	–O(15^{iii})	= 2.715(8)
–O(22)	= 2.941(8)	–O(16)	= 3.020(8)
–O(22^{viii})	= 2.941(8)	–O(16^{iii})	= 3.020(8)
		–O(17)	= 2.938(3)
		–O(17^{iii})	= 2.938(8)

Symmetry code

i	$-x$	y	$1/2 - z$
ii	$1/2 - x$	$1/2 - y$	$1/2 + z$
iii	$1 - x$	y	$1/2 - z$
iv	$1/2 - x$	$1/2 + y$	$1/2 - z$
v	$1/2 - x$	$y - 1/2$	$1/2 - z$
vi	$-1/2 + x$	$1/2 + y$	z
vii	$-1/2 + x$	$1/2 - y$	$-z$
viii	x	$-y$	$1 - z$
ix	$1/2 + x$	$1/2 + y$	z

atoms around Rb(1) and those around Rb(3) delimit identical polyhedra, but they are different from the polyhedron of K(2) delimited only by eight oxygen atoms. The Rb(2) and the Rb(4) cations are near the axis of the tunnels running respectively along **a** and **b**. Rb(2) lies in an octahedron of oxygen and Rb(4) is surrounded by eight oxygen atoms in such a way that there are two perpendicular planes containing five oxygen atoms each. These two polyhedra are very different from the one of K(1) which is a hexagonal bipyramid.

CONCLUDING REMARKS

This study confirms the possibility of a mixed valency Mo(V)–Mo(VI) "delocalized" over two corner-sharing octahedra. It opens the road to the research of other intersecting tunnel structures, intermediate between the $K_2O(MoO)_2(PO_4)_2$ structure and the $Rb_3O_2(MoO)_4(PO_4)_4$ structure, based on a chemical twinning mechanism that allows the content of the interpolated cation to be varied.

REFERENCES

1. C. Gueho, M. M. Borel, A. Grandin, A. Leclaire, and B. Raveau, *J. Solid State Chem.* **104,** 202 (1993).
2. M. F. Zid, T. Jouini, N. Jouini, and M. Omezzine, *J. Solid State Chem.* **74,** 337 (1988).
3. M. F. Zid and J. Jouini, *C.R. Acad. Sci.* **315,** 59 (1992).
4. M. M. Borel, A. Leclaire, A. Grandin, and B. Raveau, *J. Solid State Chem.*, in press.
5. W. H. Zachariasen, *J. Less Common Met.* **62,** 1 (1978).